Journal of Macromolecular Science, Part A
Publication details, including instructions for authors and subscription information:
http://www.informaworld.com/smpp/title~content=t713597274

Finite Element Analysis and Structure Optimization for Improving the Fatigue Life of Rubber Mounts

Jiancai Zhao[a]; Qian Li[a]; Xiaoyan Shen[a]
[a] School of Mechanical Engineering, Shanghai Jiao Tong University, Shanghai, P. R. China

Online publication date: 04 January 2011

To cite this Article Zhao, Jiancai , Li, Qian and Shen, Xiaoyan(2008) 'Finite Element Analysis and Structure Optimization for Improving the Fatigue Life of Rubber Mounts', Journal of Macromolecular Science, Part A, 45: 6, 479 — 484
To link to this Article: DOI: 10.1080/10601320801977780
URL: http://dx.doi.org/10.1080/10601320801977780

Journal of Macromolecular Science®, Part A: Pure and Applied Chemistry (2008) **45**, 479–484

ISSN: 1060-1325 print/1520-5738 online
DOI: 10.1080/10601320801977780

Finite Element Analysis and Structure Optimization for Improving the Fatigue Life of Rubber Mounts

JIANCAI ZHAO, QIAN LI, and XIAOYAN SHEN

School of Mechanical Engineering, Shanghai Jiao Tong University, Shanghai, P. R. China

Received November, 2007, Accepted December, 2007

The fatigue crack problem of a rubber mount on the crankshaft of a wheel in an automobile was investigated by theoretical calculation and experimental analysis. A finite element analysis (FEA) model of the rubber mount was developed and analyzed using the software MSC.MARC. FEA results imply that stress concentration may arise on the interfaces of the rubber layer and metal layer. Modifications were made to the structure parameters and rubber material of the rubber mount based on the analysis of FEA results. The stress concentration of the rubber mount at the rubber and metal interfaces was improved and the fatigue life of the improved rubber mount was increased. Finally, experiments were made to validate the accuracy of the FEA process and the reliability of the improved method. The proposed FEA and improved method can shorten the product design cycle, decrease the design and trial-product cost and remarkably improve the product quality.

Keywords: rubber mount; fatigue crack; finite element analysis (FEA); stress concentration; fatigue life

1 Introduction

As an important vibration isolation part in vehicles, rubber mounts have two functions; one is to support the static load, the other is to provide a dual damping mode passive vibration isolator to control high-amplitude, low-frequency road-induced vibrations and low-amplitude, high-frequency engine-induced vibrations and improve the ride comfort (1, 2). The periodic loads these mounts undergo will usually lead to fatigue cracks. The vibration in riding cannot be absorbed if these mounts fail; that will affect the customers' riding comfort. More severely, it can affect the normal ride of the vehicle, and induce traffic accidents and threaten the safety of customers. Thus improving the fatigue life of rubber mounts is a desirable goal for both engineers and scholars (3).

Many scholars have carried on related research on the structure and fatigue life of rubber mounts. Kim et al. (4, 5) predicted the fatigue life of the engine rubber mount by integrating the load vs. Green-Lagrange strain relation and the fatigue damage equations of the natural rubber. The load vs. Green-Lagrange strain relation was determined by the FEA of the engine mount and the fatigue damage equations were derived based on fatigue tests of dumbbell specimens. Beijers et al. (6) established a numerical cylindrical vibration isolator model with the finite element package ABAQUS. Dai et al. (7) analyzed the structure of the engine front and back suspending bearings and obtained the stress contour. Based on that, the initial position where a crack occurs was determined and the possible crack surface was pointed out. It provided reference to crack analysis and crack propagation tracking. Wang and Lu (8) investigated the static elastic character of a spring mount based on the FEA of the spring mount using the finite element analysis software ABAQUS and ADINA. Nevertheless the method to improve the fatigue life of rubber mounts has not be discussed in this research.

Figure 1 shows a diagram of a rubber mount after a fatigue crack. To solve the fatigue crack problem of the rubber mount on the crankshaft of a vehicle wheel in driving travel and increase the fatigue life of the rubber mount, the stress distribution of the rubber mount was analyzed using the FEA method. The critical regions, which are prone to develop cracks, were predicated based on FEA results. Modifications were made to the structure parameters and rubber material. Finally, the reliability of the improved method was validated by the FEA and experimental methods.

Address correspondence to: Jiancai Zhao, School of Mechanical Engineering, Shanghai Jiao Tong University, Shanghai 200240, P. R. China. Tel.: +86-21-34206316; Fax: +86-21-34206515. E-mail: zhaojc@sjtu.edu.cn

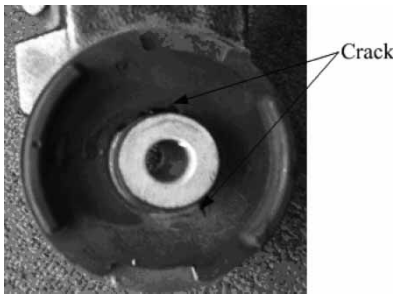

Fig. 1. Photo of the rubber mount after fatigue crack.

2 Experimental

2.1 The Hyperelastic Constitutive Model of the Natural Rubber Material

The natural rubber can be considered as a hyperelastic material, showing highly nonlinear elastic isotropic behavior with incompressibility (4). A relationship between stress and strain in the hyperelastic material, generally characterized by strain energy potentials, is essential for the FEA of rubber components. In order to define the hyperelastic material behavior, i.e., the constitutive relation, experimental test data are required to determine material parameters in the strain energy potential.

The Mooney-Rivlin function was selected to specify the constitutive model of the natural rubber material in this study. The strain energy potential of the Mooney-Rivlin model can be expressed as Equation (1).

$$W = \sum_{i+j=1}^{N} C_{ij}(I_1 - 3)^i(I_2 - 3)^j + \frac{1}{2}k(\sqrt{I_3} - 1)^2 \qquad (1)$$

Where C_{ij} is a material parameter determined by the material test, k is the volume modulus, I_1, I_2, and I_3 are the first, second, and third order invariable strain values, respectively. I_1, I_2, and I_3 can be calculated from the principal stretch ratios λ_1, λ_2, and λ_3, which are defined as the ratio of the extended length of a specimen to the original length of the specimen in three principal stress directions.

$$I_1 = \lambda_1^2 + \lambda_2^2 + \lambda_3^2 \qquad (2)$$

$$I_2 = (\lambda_1\lambda_2)^2 + (\lambda_2\lambda_3)^2 + (\lambda_1\lambda_3)^2 \qquad (3)$$

$$I_3 = (\lambda_1\lambda_2\lambda_3)^2 \qquad (4)$$

In the uniaxial stress state, the principal stretch ratios λ_1, λ_2, and λ_3 are expressed as Equation (5).

$$\lambda_1 = \lambda_u, \lambda_2 = \lambda_3 = 1/\sqrt{\lambda_1} \qquad (5)$$

Where λ_u is the principal stretch ratio in the loading direction, λ_2 and λ_3 are the principal stretch ratios on the planes perpendicular to the loading direction.

The one parameter Mooney-Rivlin model can be derived as follows:

$$W = C_{10}(\mathrm{I}_1 - 3) \qquad (6)$$

The two parameter Mooney-Rivlin model can be expressed as follows:

$$W = C_{10}(I_1 - 3) + C_{01}(I_2 - 3) \qquad (7)$$

The three parameter Mooney-Rivlin model can be expressed as follows:

$$W = C_{10}(I_1 - 3) + C_{01}(I_1 - 3) + C_{11}(I_1 - 3)(I_2 - 3) \qquad (8)$$

The three parameter Mooney-Rivlin model was selected to specify the constitutive model of the natural rubber. The moduli C_{10}, C_{01}, and C_{11} can be determined from uniaxial tensile tests of the natural rubber material. By data fit using the data acquired in uniaxial tensile tests we determined that C_{10}, C_{01}, and C_{11} were 0.581, 0.320, and 0.013, respectively. Figure 2 shows the stress vs. strain curves of the experimental data and the Mooney model data fit.

2.2 Fatigue Test

In order to compare the fatigue life between the existing mount and the improved mount and validate the effectiveness of the improvement, fatigue tests were conducted on the MTS vibration test bench. The rubber mounts were vibrated with a sine wave drive with amplitude $\pm$10000 N and frequency 5 HZ. The experiment ends when the rubber layer of the mount cracks with the number of recycles recorded.

2.3 Static and Dynamic Properties Test

The static and dynamic properties of the improved mount were measured on the MTS 831 elastomer test system to determine whether the static and dynamic properties of the improved robber mount are consistent with the design requirement. The improved rubber mount was fixed on the

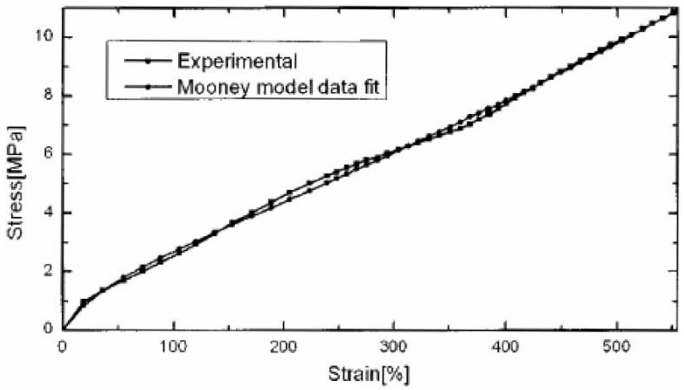

Fig. 2. The stress vs. strain curves of the rubber material.

Table 1. Test items and conditions

Item	Condition
Radial static stiffness measurement	Compress the rubber mount from 0 N to 4000 N, then release, measure the force and displacement, calculate the stiffness between 1000 N and 2000 N.
Radial dynamic stiffness and loss angle	Static preload −750 N, frequency 15 Hz, amplitude 1 mm, measure the dynamic stiffness and loss angle.

upper and bottom pole of the test system by a custom clamp. The bottom pole was fixed on the base of the test system and a load cell was installed on the upper pole. The load cell can be driven with different frequencies and amplitudes. The force transducer on the bottom pole measures the force response for the different drives. Table 1 lists the test items and conditions.

3 Results and Discussion

3.1 Computer Simulation

3.1.1 Forces Acting on the Rubber Mount

Figure 3 shows a diagram of the installation of a rubber mount on the chassis. The rubber mount is installed on the right end of a crankshaft. The left end of the crankshaft connects with the vehicle wheel and the right end of the crankshaft connects with the automobile chassis. Since the crankshaft is bent, the axis of the rubber mount on this crankshaft is 17 degrees inclined to the horizontal line, as shown in Figure 4.

Presume the biggest vertical load acting on the mount is F. According to the force decomposition principle, the vertical force F can be decomposed into two forces. The radial one is much larger than the axial one, so only the radial force was considered in the FEA of the rubber mount.

3.1.2 Finite Element Modeling and Calculation

The rubber mount investigated in this research is a ring with the cross section plane shown in Figure 5. Since

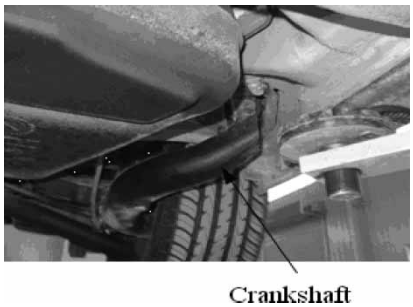

Fig. 3. Installation mode of the rubber mount.

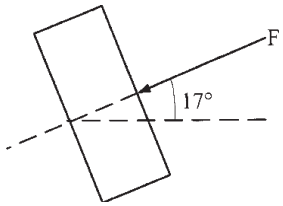

Fig. 4. The angle of the rubber mount axis to horizontal line.

the section plane is axis-symmetric, the left half of the plane was selected for finite element modeling. Although the three-dimensional problem changes into a two-dimensional plane problem, this model still reflects the geometric properties of the part by giving the model a thickness value during geometric property setting in the MARC software.

The model can be meshed into three layers in the mesh generation in MARC. The first layer is the outer bushing layer with the material AlSiMnZn. The second layer is the natural rubber layer with natural rubber NR50, whose Shore hardness is 50. The third layer is the inner bushing layer in the material $AlMg_3$. The four nodes planar element was selected for the model. The Advanced Front Quad tool was selected to generate elements automatically (9). The inner bushing layer, middle rubber layer and outer bushing layer were meshed into 1482, 3669, and 400 elements, respectively. Edge load, equal to 114 N/mm, acts on the outer bushing layer. Since the rubber mount is fixed on the crankshaft by the inner bushing, the displacement of the exterior edge of the inner layer in X, Y, and Z direction was defined as 0. Figure 6 is the finite element model of the rubber mount in MARC.

FEA results are shown in Figure 7. It can be seen from the figure that the maximum strain in areas A, B, C, and D are 49%, 37%, 37%, and 62%, respectively. The stress concentration in areas A and D is very obvious. Thus, we conclude that the crack is most likely to arise in area A or D, that is, the interfaces of the rubber and metal layers, which agrees well with the real crack position shown in Figure 1.

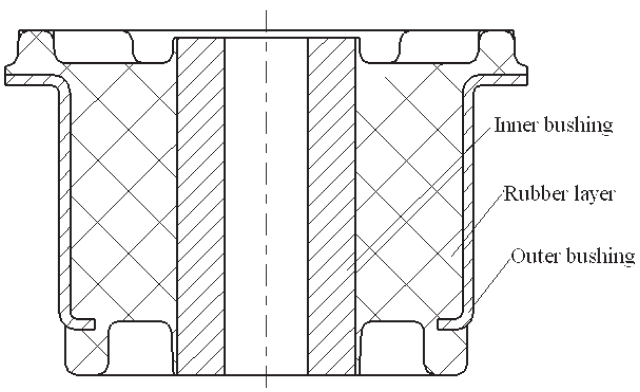

Fig. 5. The cross section of the rubber mount.

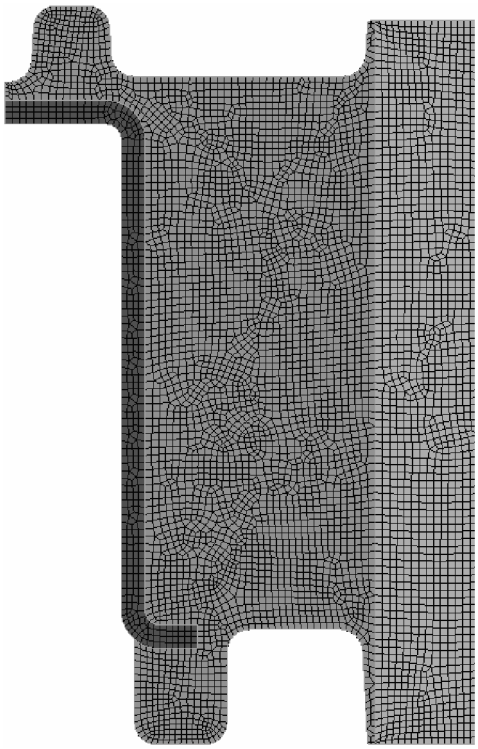

Fig. 6. The finite element model of the rubber mount.

3.2 Improvement Methods and the FEA of the Improvement Methods

To improve the stress concentration at the interfaces of rubber and metal layer and increase the fatigue life of the rubber mount five improved methods including three improved methods to structure and two improved methods to rubber material are proposed and analyzed.

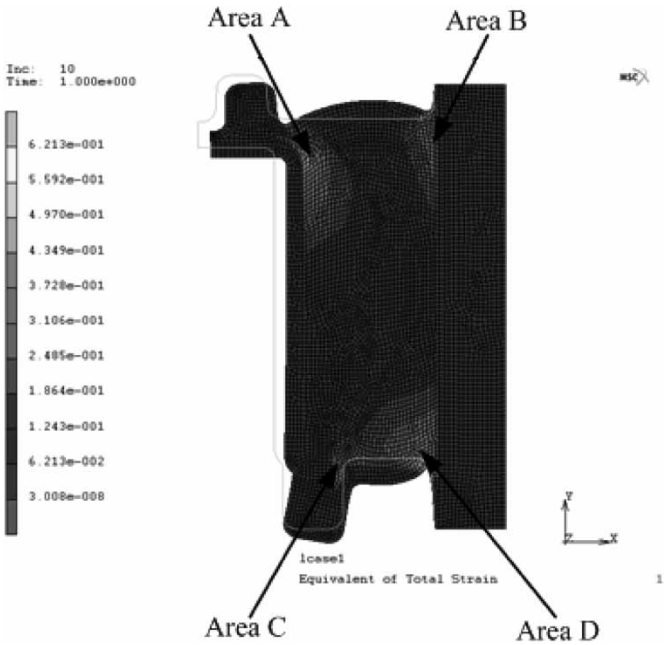

Fig. 7. The strain contour of the rubber mount.

3.2.1 Structure Improvements and the FEA of the Rubber Mounts After Structure Improvements

Three structure improvement methods are proposed. The configurations are shown in Figure 8 and Table 2.

FEAs were also made of the rubber mounts after the structure improvements. Table 3 lists the maximum strain in areas A, B, C, and D of the original rubber mounts and the improved rubber mounts.

It can be seen from Table 3 that the best method is method 2; the maximum strain in area A of the rubber mount, after being improved by method 2, decreases from 49% to 43%, the maximum strain in area B decreases from 37% to 34% and the maximum strain in area D decreases from 62% to 43%. The maximum strain in areas A and D of the rubber mount, after being improved by method 2, is much less than that of the original rubber mount. Changing the shape of the inner bushing is the most effective improvement method.

3.2.2 Material Improvement and the FEA of the Rubber Mounts After Material Improvements

In order to compare the influence of different materials on the strain contour of the rubber mount, rubber material changes were made to the rubber mounts after improvement by changing the shape of the inner bushing. The original rubber material was replaced by NR45 and NR60, which are natural rubbers with Shore hardness 45 and 60. The FEA results of rubber mounts with rubber materials NR45 and NR60 are shown in Table 4.

The maximum strain in areas A, B, C, and D of the rubber mounts with the rubber material NR45 and NR50 are almost same. The maximum strain in areas A, B, C, and D of the rubber mount with rubber material NR60 is much less than that of rubber mounts with the rubber materials NR45 and NR50.

According to the analysis results, changing the shape of the inner bush and using the rubber material NR60 was adopted as the final improvement method.

3.3 Experimental Analysis

3.3.1 The Analysis of Fatigue Test Results

Five samples of the improved rubber mount were manufactured in this study. The fatigue test of the original mount ended after 7651 cycles, while the fatigue test of the improved mount samples on an average ended after 42,911 cycles. The average fatigue life of the improved mount was 5.6 times that of the original mount.

3.3.2 The Analysis of Static and Dynamic Properties Test Results

The design requires that the radial stiffness between 1000 N and 2000 N is in the 900–2700 N/mm range, the dynamic

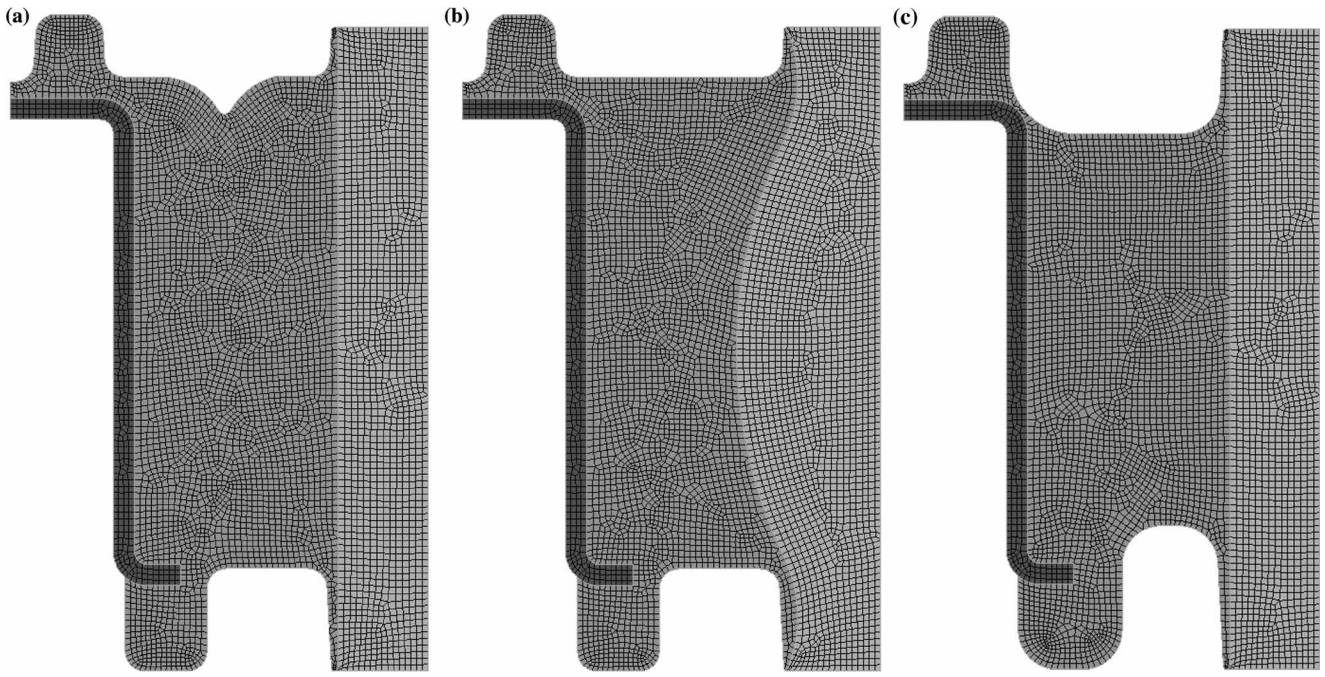

Fig. 8. Improvement schemes of the rubber mount (a) Method 1, (b) Method 2, and (c) Method 3.

stiffness at 15 Hz is in the 510–600 N/mm range, and the loss angle at 15 Hz is in the 4–7 degree range. According to the load vs. displacement curve shown in Figure 9, the radial stiffness between 1000 N and 2000 N was 2564.1 N/mm. The dynamic stiffness and loss angle at 15 Hz were 583.7 N/mm and 5.9 degree, respectively. The static stiffness, dynamic stiffness and loss angle are all consistent with the design requirement. From the above experimental data, we can conclude that the improved rubber mount can not only increases the fatigue life but also ensures that the static and dynamic stiffness satisfy the design requirement.

Table 2. Improvement methods to the structure of rubber mount

Improvement method no.	Improvement method
1	Dig groove in the rubber layer. See as Fig. 8(a).
2	Change the shape of the inner bush. See as Fig. 8(b).
3	Enlarge the load-discharged groove. See as Fig. 8(c).

Table 3. Maximum strain in areas A, B, C, and D of the original rubber mount and the improved rubber mounts

Improvement method no.	Max strain in area A	Max strain in area B	Max strain in area C	Max strain in area D
1	49%	35%	35%	63%
2	43%	34%	38%	43%
3	62%	41%	34%	62%
Original rubber mount	49%	37%	37%	62%

Table 4. The maximum strain of rubber mounts with different rubber materials in areas A, B, C, and D

Rubber material	Max strain in area A	Max strain in area B	Max strain in area C	Max strain in area D
NR45	42%	34%	38%	42%
NR50	43%	34%	38%	43%
NR60	28%	21%	21%	28%

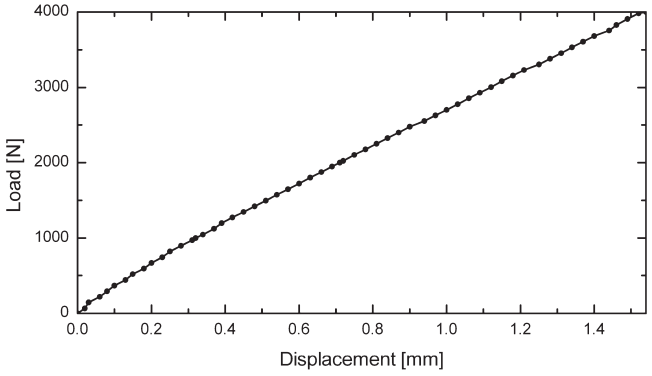

Fig. 9. The load vs. displacement curve of the improved rubber mount.

4 Conclusions

The main reason for fatigue cracking of the rubber mount is stress concentration and the regions, which are prone to develop cracks, are the interfaces between the rubber and metal layers. Changing the shape of the inner bushing and using harder rubber material, NR60, can decrease the stress concentration at the interfaces the rubber and metal layers. Fatigue life of the improved rubber mount was increased from 7651 cycles to 42911 cycles, which is 5.6 times that of the original rubber mount; thus the improvement method is effective.

5 Acknowledgments

We are grateful to the Ninghai Jianxin Rubber and Plastic Parts Co., Ltd., PR China for making the experimental studies possible by providing the MTS Elastomer Test System and components.

6 References

1. Christopherson, J., Jazar, G. and Nakhaie (2006) *J. Sound. Vibr.*, **290(3–5)**, 1040–1070.
2. Kim, G. and Singh, R. (1995) *J. Sound. Vibr.*, **179(3)**, 427–453.
3. Mars, W.V. and Fatemi, A. (2002) *Int. J. Fatigue*, **24(9)**, 949–961.
4. Kim, W.D., Lee, H.J. and Kim, J.Y. (2004) *Int. J. Fatigue*, **26(5)**, 553–560.
5. Woo, Chang-Su, Kim, Wan-Doo, Kwon and Jae-Do. (2007) *Mat. Sci. Eng. A-Struct.*, doi:10.1016/j.msea.2006.09.189.
6. Beijers, Clemens, A.J., De Boer, and Andre. (2003) Proceeding of the Tenth International Congress on Sound and Vibration, 805–812.
7. Dai, Yongqian, Song, Xigeng, Xue, and Dongxin. (2005) *Chinese J. Agriculture. Mech.*, **36(10)**, 23–25.
8. Wang, Lirong, Lu, and Zhenhua. (2002) *Chinese J. Automobile. Eng.*, **12(6)**, 481–485.
9. MARC Analysis Research Corporation. MARC user's manual. Chapt. 2–7, 1996.